Journal of the Brazilian Society of Mechanical Sciences and Engineering (2018) 40:329
https://doi.org/10.1007/s40430-018-1253-y

TECHNICAL PAPER

Rapid thermal cycling of three phase change materials (PCMs) for cooking applications

A. B. Shobo[1] · A. Mawire[2] · M. Aucamp[3]

Received: 3 July 2017 / Accepted: 28 May 2018 / Published online: 5 June 2018

Abstract
The suitability of the use of acetanilide, meso-erythritol and In-48Sn as phase change materials (PCMs) in latent heat thermal storage systems (LHTES) for cooking applications has been investigated under high charging and heat retrieval conditions. In-48Sn showed the greatest thermal stability up to 289.68 °C with meso-erythritol showing stability up to 177.03 °C, while acetanilide is thermally stable up to 133.33 °C. Thermal properties of acetanilide remained within stable limits with rapid thermal cycles, but rapid mass degradation was observed. Two forms of meso-erythritol were manifested with different melting points with the solidification temperature that showed considerable variations while the enthalpy of solidification remained reasonably stable. Acetanilide and meso-erythritol exhibited large degrees of supercooling below 100 °C making them undesirable to be used in a LHTES unit for cooking applications under rapid heating and cooling cycles. With the solidification temperature of In-48Sn above 100 °C throughout the thermal cycles, it proved to be a promising PCM for cooking applications under rapid heating and cooling cycles. The residues of the PCMs after thermal cycling showed no structural changes as compared with the fresh samples while the health hazards related to the PCMs were all within acceptable limits. Though the cost implication of utilizing In-48Sn is much higher as compared with the other two PCMs, its good cycling stability and its average solidification temperature being within desired cooking temperature makes it a preferred PCM candidate under fast heat retrieval condition than acetanilide and meso-erythritol.

Keywords Phase change materials (PCM) · Thermal stability · Cycling stability · Acetanilide · Meso-erythritol · In-48Sn

1 Introduction

The application of phase change materials (PCMs) in latent heat thermal storage systems for the storage of solar thermal energy and waste heat for various temperature applications has been widely explored in the past few years. PCMs in latent heat thermal storage (LHTES) systems have advantages of large energy storage densities due to the large amounts of thermal energy that can be stored and retrieved during their phase change transitions. The solid–liquid phase change transitions of PCMs are particularly of interest due to their great efficiencies and larger enthalpies associated with these transitions [1]. The isothermal/near-isothermal behavior of PCMs during heat storage or heat retrieval processes is also attractive for some temperature-controlled applications. Therefore, for a particular application, the melting and the solidification temperatures of the PCM to be utilized are of paramount importance. Due to the possibility of the existence of many PCM candidates with phase transition temperatures about the desired temperature application, many other properties need to be considered for choice of the suitable PCM. These properties include: density, specific heat capacity, latent heat of fusion, thermal conductivity, degree of supercooling, thermal stability, cycling stability, toxicity, degree of

Technical Editor: Jose A. R. Parise.

✉ A. B. Shobo
adetumirola@gmail.com

[1] Department of Mathematics, Science and Sports Education, University of Namibia, Private Bag 5507, Oshakati, Namibia

[2] Department of Physics and Electronics, Northwest University (Mafikeng Campus), Private Bag X2046, Mmabatho 2735, South Africa

[3] Faculty of Health Sciences, Center of Excellence for Pharmaceutical Sciences, Northwest University (Potchefstroom Campus), Private Bag X6001, Potchefstroom 2520, South Africa

health hazard, compatibility with containment material, abundance and cost [2, 3].

Thermal energy storage by indirectly heating a PCM in a LHTES unit for solar cooking has been reported to provide the convenience of indoor cooking [4]. In this mode, a suitable heat transfer fluid (HTF) transports thermal energy from a solar collector to the LHTES unit where it exchanges heat with the PCM. The PCM first absorbs sensible heat and then on attaining its melting temperature, it absorbs the enthalpy of fusion over a narrow range of temperature. For the utilization of the stored thermal energy, the HTF is also used to transport the thermal energy from the LHTES unit to the cooking unit as the PCM solidifies. The thermal energy from the LHTES unit must be able to bring the food to boil and sustain the boiling for a length of time depending on the food type. Studies have recommended that PCMs with melting temperatures higher than 100 °C should be used in heat storages for efficient cooking applications [5, 6]. It is important for cooking applications that the PCM's solidification temperature should be slightly higher than 100 °C so that the released solidification enthalpy will be used to just maintain the cooking of food at about that same temperature. Since cooking of food is a daily routine, the PCM utilized in a thermal storage for this purpose should also exhibit good thermal cycling stability. Particular attention also needs to be paid to the degree of the health hazard posed by the PCM used in thermal storage systems for cooking applications [3].

Only organic and inorganic PCMs have been utilized LHTES systems designed for cooking as found in the available literature [4, 7, 8]. Table 1 shows a list of some of the PCMs that had been previously utilized as thermal storage materials for cooking applications from the literature.

Common problems that are associated with organic and inorganic PCMs, however, include low thermal conductivity, supercooling and thermal instability [16]. In order to avoid these outlined problems, the use of metals and metal alloys as PCM has been suggested by a number of studies [17, 18]. The outlined advantages of metallic PCMs include high thermal conductivity, large volumetric enthalpy of fusion, large heat capacity and good stability after several melting/solidification cycles. It is therefore important to investigate possible metallic PCMs that may be used in thermal energy storage systems for cooking applications. Considerable numbers of studies have investigated the use of metallic PCMs for high-temperature applications, but limited studies are available on medium-temperature applications like cooking [17].

Acetanilide has been identified by a number of studies as a PCM for latent thermal energy storage systems for temperature applications between 110 and 120 °C [2, 19, 20]. Acetanilide has been utilized as a PCM for thermal energy storage for cooking applications in some published studies [7, 9, 21]. El-Sebaii et al. [22] presented a study involving fast thermal cycling of acetanilide for 500 cycles. Results showed that the melting temperature and latent heat of fusion decreased after 500 cycles. They concluded that acetanilide showed good thermal stability and is thus a promising PCM for the storage of solar thermal energy for indoor cooking. The study by El-Sabaii and Al-Agel [23] reported 15 °C supercooling of acetanilide during 1000 melting/solidification cycles and also concluded that acetanilide is a promising PCM for thermal energy storage.

Erythritol has also been identified by several studies as a PCM for latent heat thermal energy storage systems for temperature applications between 110 and 120 °C [24–29]. Sharma et al. [10] utilized erythritol as a heat storage material in a heat storage unit designed for cooking application. The study by Kaizawa et al. [25] reported that erythritol began to decompose at 160 °C and as such its maximum charging temperature for heat storage should be less than 160 °C. Shukla et al. [30] presented an accelerated thermal cycling test of erythritol and results indicated no degradation of erythritol during 75 thermal cycles while the degree of supercooling of 15 °C was observed.

In-48Sn is an alloy of indium and tin with a composition of 52% indium and 48% tin by weight. It is commonly used as a low-melting-temperature solder in electronic circuit construction. The only application of the alloy as a PCM, found in the literature, is for heat dissipation as an

Table 1 List of PCMs previously used as thermal storage materials for cooking applications

PCM	Melting temperature (°C)	Melting enthalpy (kJ/kg)
Acetamide [5]	82.0	263.0
Acetanilide [9]	118.9	222.0
Erythritol [10]	118.0	339.8
$Mg(NO_3)_2{\cdot}6H_2O$ [11]	89.0	134.0
$NaNO_3$-KNO_3 [12]	210.0–220.0	N.A.
Paraffin [13]	100.0	140.0
Polyethylene [14]	126.0	235.0
Stearic acid [15]	55.1	160.0

encapsulation material for an electronic module in the invention of Myers et al. [31]. There is no literature presenting the thermal and cycling stability of this alloy for use as a PCM for heating applications.

For large-scale acceptance of solar cookers integrated with thermal energy storage systems, they must be able to provide the convenience and the flexibility offered by conventional cooking energy sources for adaptation in different user-defined cooking operations. Thus, it is reasonable to investigate PCMs under different working conditions related to potential end uses. This is because the potential end user of a LHTES system may desire to subject it to very high charging rates for cooking applications which may require very high heat retrieval rates. The reported thermal cycling studies of acetanilide and erythritol [22, 23, 30] in the literature have been conducted at lower heating/cooling rates than the scenario presented in this study. The mass degradations of both PCMs during the previously reported thermal cycling experiments were not considered as well as effects on their solidification enthalpies. For the reliability and predictability of the performance of a LHTES unit, having the knowledge of any potential mass degradation of the PCM and the variability of the solidification enthalpy is essential.

The objective of this paper is to investigate the suitability of the use of acetanilide, meso-erythritol and In-48Sn as PCMs in a LHTES system for cooking applications under fast charging and heat retrieval conditions. Additionally, the potential of using In-48Sn as a metallic PCM in LHTES systems for cooking applications will be investigated in this study.

2 Materials and methods

2.1 Materials

The materials investigated in this research are commercial grade acetanilide (purity 98%) purchased from Alfa Aeser GmbH & Co.KG, Germany [32]. Commercial grade meso-erythritol (purity 99.92%) was purchased from J&K scientific, China [33] and a commercial grade In-48Sn ingot (purity 99.9%) was purchased from the Indium Corporation of America, USA [34].

2.2 Methods

Tests of thermal and cycling stabilities were conducted on the SDT Q600 simultaneous thermal analyzer (TA instrument, Delaware, USA), which is a dual-purpose thermogravimetric analyzer (TGA) (error: $\pm$ 0.1 µg) and a differential scanning calorimeter (DSC) (calorimetric accuracy = $\pm$ 2%, DTA sensitivity = 0.001 °C). It thus measures simultaneously weight changes and heat flow in a material with respect to temperature and time, under a controlled atmosphere. Thermal stability tests of the PCMs were done with a heating rate of 10 °C/min in open, 90 µl alumina pans under a 50 ml/min flow of nitrogen. For the test of cycling stability, each PCM sample was subjected to 20 rapid heating/cooling rates at 20 °C/min from a temperature below their observed solidification temperature to a temperature below their observed decomposition temperature. The cycling tests were conducted with each PCM sample in 90-µl alumina pans, under a 20 ml/min flow of nitrogen.

The chemical stability of each of the PCM was investigated by comparing infrared spectra obtained before and after the thermal cycling. The spectra were recorded on a Cary 670 FTIR spectrometer (Agilent Technologies, California, USA) from 600 to 4000 cm^{-1}. Spectral acquisitions were done using Essential FTIR v.3.50.083 (Operant LLC, USA). Due to the insufficient data about the thermophysical properties of In-48Sn, the specific heat capacity of In-48Sn was measured using a differential scanning calorimeter (DSC 204 F1 Phoenix, NETZSCH with a precision $<$ 2–3%). The density of the In-Sn alloy at room temperature was obtained by a buoyancy method while the density at elevated temperatures was obtained from the thermal expansion measurements which were obtained by using a push-rod dilatometer (DIL 402C, NETZSCH with measurement error $<$ 3%).

The degree of health hazard of each material is obtained from the material datasheet provided by the manufacturer of each of the material tested.

3 Results and discussion

3.1 Thermal stability tests

Figure 1a–c shows the DSC-TGA thermograms obtained for acetanilide, meso-erythritol and In-48Sn at a heating rate of 10 °C/min. Decomposition of acetanilide was observed to commence at about 133.33 °C which is taken as the point where the curve for the first derivative of weight with temperature begins to rise (Fig. 1a). However, decomposition of In-48Sn is noticed at about 289.68 °C, where the first derivative of the weight with respect to temperature shows a peak. Decomposition of meso-erythritol commenced at about 177.03 °C. In-48Sn may therefore be safely utilized in a LHTES system charged up to about 289.7 °C, higher than temperatures at which acetanilide (133.3 °C) and meso-erythritol (177.0 °C) may be charged. At about 230 °C, acetanilide had decomposed to about 20% of the original mass present while just about

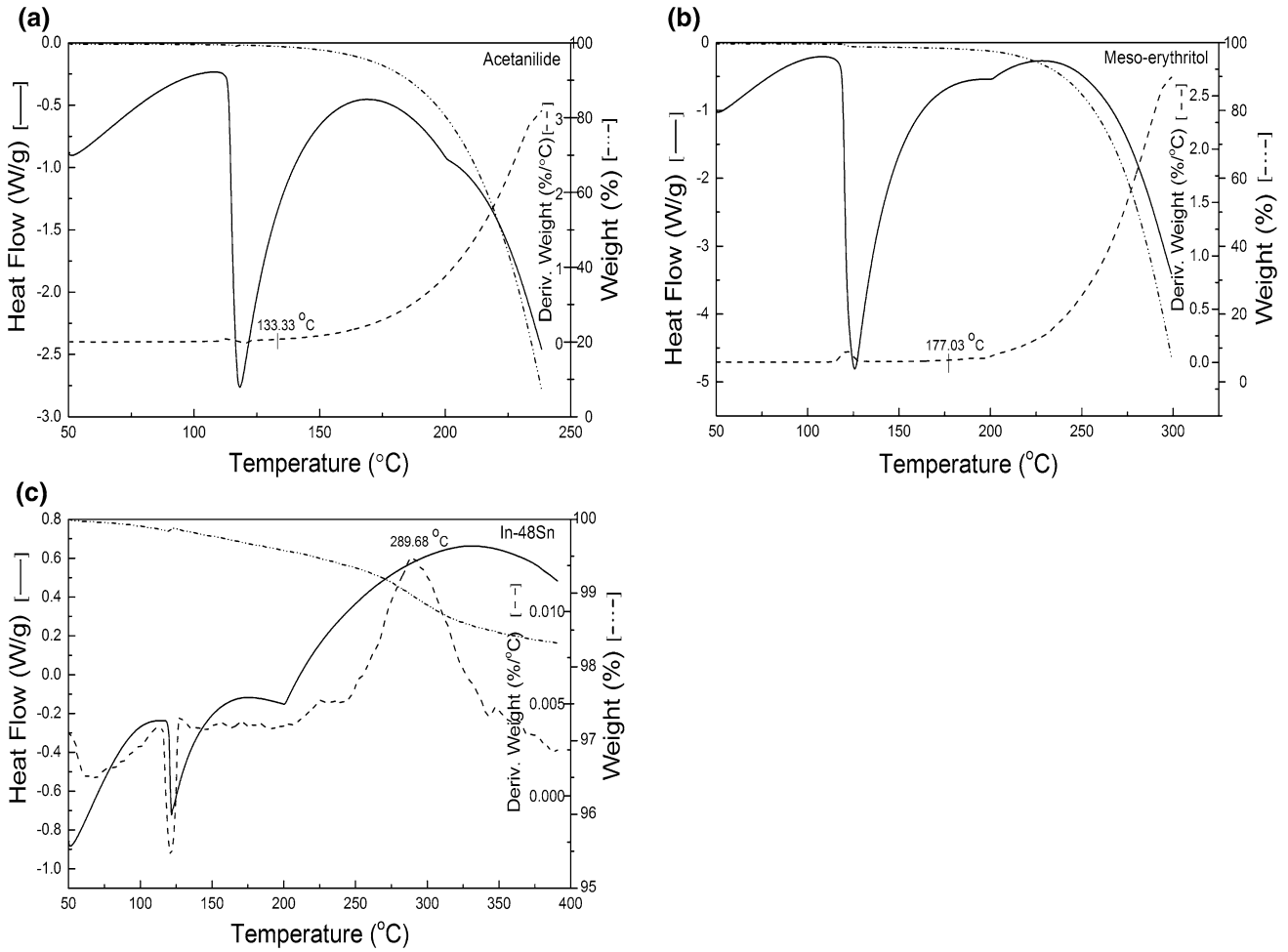

Fig. 1 TGA–DSC thermograms of **a** acetanilide, **b** meso-erythritol and **c** In-48Sn at a heating rate of 10 °C/min

6% of meso-erythritol had decomposed and a mere 0.5% mass degradation was shown in the In-48Sn sample.

3.2 Thermal cycling tests—DSC

The DSC heat flow thermograms obtained for the cycling stability tests for acetanilide, meso-erythritol and In-48Sn at heating/cooling rates of 20 °C/min, respectively, are shown in Fig. 2a–c. Acetanilide was thermally cycled between 35 and 130 °C, meso-erythritol between 20 and 140 °C and In-48Sn between 35 and 140 °C. The melting and solidification onset temperatures were determined by the point of intersection of the tangent to the point of maximum slope of the leading edge of the heatflow peaks with the extrapolated baseline. The peak melting and solidification temperatures were obtained by drawing a line at the point of maximum slope of the leading edge of the DSC peak and extrapolating the baseline on the same side of the leading edge of the peak. The solidification enthalpies of the PCMs were obtained by numerically integrating the area under the weight-corrected solidification peak and the extrapolated baseline by using the TA instruments' Universal analysis 2000 software. The melting onset temperatures ($T_{m,\ onset}$), the melting peak temperatures ($T_{m,\ peak}$), the solidification onset temperatures ($T_{s,\ onset}$), the solidification peak temperatures ($T_{s,\ peak}$), solidification enthalpies (ΔH_s) and the relative percentage difference (RPD) of each these properties obtained for each of the PCM at each thermal cycle are recorded in Tables 2, 3 and 4. The RPD of a PCM's property in this study is defined as the percentage difference between the value of that property at a thermal cycle and that at cycle 1.

From Table 2, it can be observed that the melting temperature of acetanilide varied between − 0.02 and − 0.73% of the initial value of 113.77 °C. The melting peak temperature varied between − 1.05 and 0.39% of the initial value of 118.52 °C. Not much significant variation was observed in the melting onset and peak temperatures. Larger variations of between − 3.83 and 2.79% of the initial value of 72.73 °C were observed in the solidification onset temperature. The solidification peak temperature also

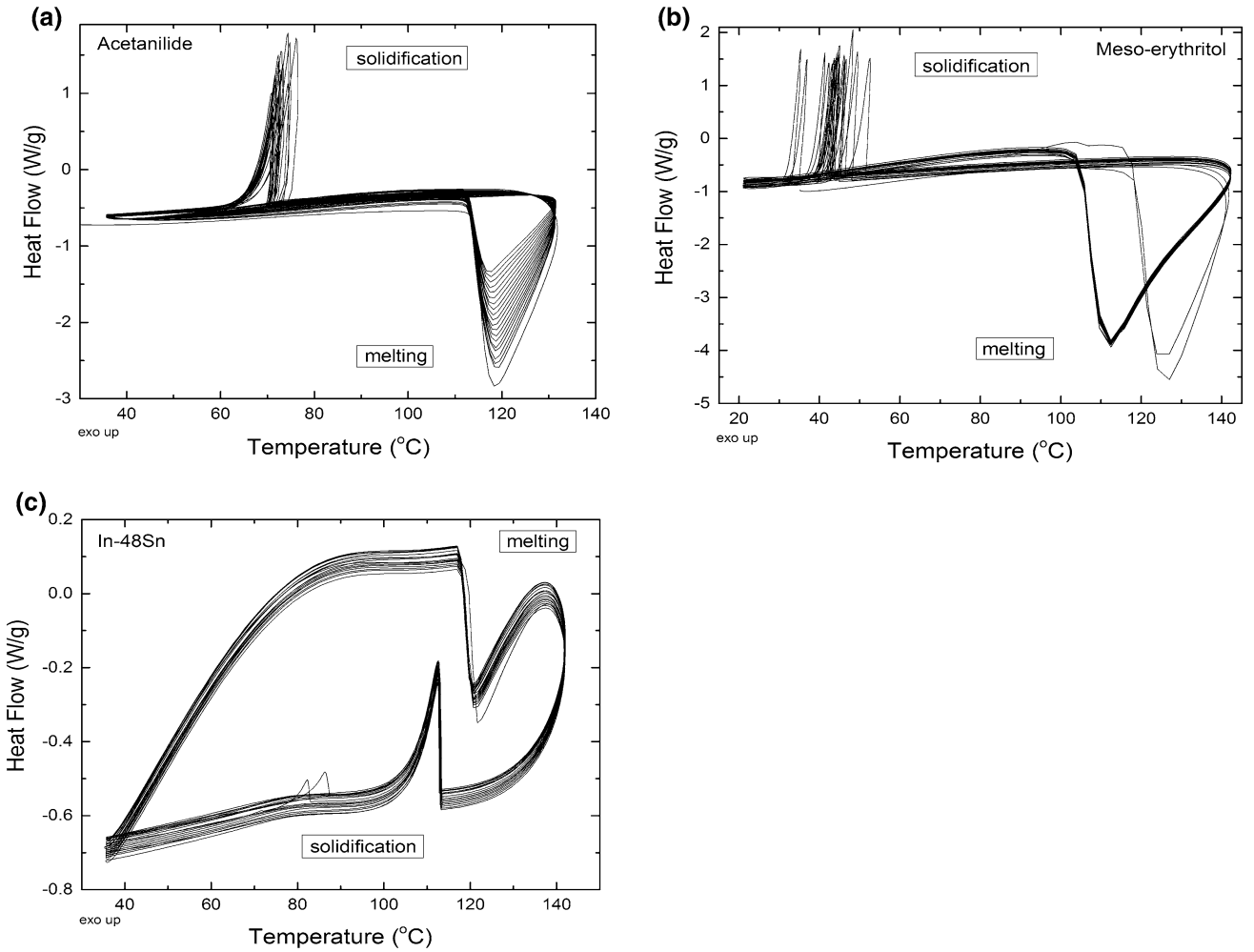

Fig. 2 DSC thermograms of **a** acetanilide, **b** meso-erythritol and **c** In-48Sn alloy for 20 heating and solidification cycles at heating/cooling rates of 20 °C/min

showed corresponding variations of between − 5.32 and 2.59% from the initial value of 79.39 °C.

The solidification enthalpy showed variations of between − 1.56 and 0.57% of the initial value of 141.1 J/g which is not significant and the variations followed no particular trend. It can therefore be concluded that these thermophysical properties of acetanilide remain within stable limits over several thermal cycles which is in agreement with the conclusion reached by El-Sabaii et al. [23]. Acetanilide also exhibited degrees of supercooling from between 38.55 and 43.36 °C through the 20 heating/solidification cycles.

The melting onset and peak temperatures for meso-erythritol showed a very big leap from 119.18 to 125.73 °C in the first cycle to 105.05 and 112.80 °C, respectively, in the second cycle as can be observed from Table 3. The melting onset temperature then showed a slightly increasing trend from about + 0.09% to about 0.32% of 105.05 °C until the seventeenth cycle when it leaped up to 117.81 °C.

The melting peak temperature showed a slightly decreasing trend from about − 0.12% to about − 0.99% of 112.80 °C until the seventeenth cycle when it also leaped to 125.10 °C. The onset and peak temperature then reduced drastically again to 105.38 and 111.68 °C. Rapid cooling of erythritol has been reported by Jesus et al. [35], to result in a polymorphic transformation into an amorphous form which is metastable with a melting temperature of about 104 °C.

This was explained to be due to an amorphous solid erythritol obtained from melt, bypassing a solid–solid transition when heated again. The solidification onset temperature showed large variations of between 5.67 and 55.79% from the value in cycle 1. The solidification peak temperature likewise showed large variations of between 4.38 and 48.61% of the value in cycle 1. It can be observed that the solidification onset and peak temperatures did not

Table 2 Melting range, solidification range and enthalpy of solidification of acetanilide obtained for each thermal cycle on the DSC

Cycle no.	$T_{m,\ onset}$ (°C)	RPD (%)	$T_{m,\ peak}$ (°C)	RPD (%)	$T_{s,\ onset}$ (°C)	RPD (%)	$T_{s,\ peak}$ (°C)	RPD (%)	ΔH_s (J/g)	RPD (%)
1	113.77	–	118.52	–	72.37	–	74.39	–	141.10	–
2	112.94	− 0.73	118.98	0.39	74.39	2.79	76.31	2.59	141.80	0.50
3	112.93	− 0.06	118.72	0.17	72.90	0.73	74.81	0.57	141.50	0.28
4	112.92	− 0.07	118.62	0.08	71.20	− 1.62	73.05	− 1.81	141.90	0.57
5	112.94	− 0.05	118.87	0.30	70.66	− 2.36	72.36	− 2.74	140.30	− 0.57
6	112.93	− 0.06	118.60	0.07	70.77	− 2.21	72.48	− 2.58	140.10	− 0.71
7	112.95	− 0.04	118.50	− 0.02	71.83	− 0.75	73.35	− 1.41	140.30	− 0.57
8	112.98	− 0.02	118.61	0.08	71.20	− 1.62	72.71	− 2.27	139.60	− 1.06
9	112.97	− 0.03	118.50	− 0.02	70.24	− 2.94	71.69	− 3.65	140.30	− 0.57
10	112.97	− 0.03	118.21	− 0.26	70.45	− 2.65	71.86	− 3.42	140.50	− 0.43
11	112.96	− 0.04	118.31	− 0.18	73.22	1.17	74.45	0.08	138.00	− 2.20
12	112.96	− 0.04	118.21	− 0.26	69.60	− 3.83	70.91	− 4.70	139.00	− 1.49
13	112.95	− 0.04	118.19	− 0.28	71.20	− 1.62	72.34	− 2.77	140.70	− 0.28
14	112.95	− 0.04	118.11	− 0.35	71.20	− 1.62	72.15	− 3.03	140.00	− 0.78
15	112.96	− 0.04	117.76	− 0.64	70.24	− 2.94	71.26	− 4.23	140.00	− 0.78
16	112.93	− 0.06	117.98	− 0.46	69.92	− 3.39	70.87	− 4.76	140.00	− 0.78
17	112.97	− 0.03	117.66	− 0.73	70.13	− 3.10	71.08	− 4.47	139.10	− 1.42
18	112.93	− 0.06	117.66	− 0.73	70.24	− 2.94	71.08	− 4.47	138.90	− 1.56
19	112.94	− 0.05	117.44	− 0.91	69.70	− 3.69	70.45	− 5.32	139.50	− 1.13
20	112.94	− 0.05	117.28	− 1.05	70.34	− 2.81	71.08	− 4.47	140.00	− 0.78

Table 3 Melting range, solidification range and enthalpy of solidification of meso-erythritol obtained for each thermal cycle on the DSC

Cycle no.	$T_{m,\ onset}$ (°C)	RPD (%)	$T_{m,\ peak}$ (°C)	RPD (%)	$T_{s,\ onset}$ (°C)	RPD (%)	$T_{s,\ peak}$ (°C)	RPD (%)	ΔH_s (J/g)	RPD (%)
1	119.18	–	125.73	–	32.98	–	35.36	–	213.10	–
2	105.05	− 11.86	112.80	− 10.28	34.85	5.67	36.91	4.38	216.50	1.60
3	105.14	− 11.78	112.67	− 10.39	40.69	23.38	42.35	19.77	219.80	3.14
4	105.21	− 11.72	112.55	− 10.48	42.56	29.05	44.16	24.89	221.80	4.08
5	105.28	− 11.66	112.44	− 10.57	44.55	35.08	46.18	30.60	223.60	4.93
6	105.31	− 11.64	112.18	− 10.78	46.41	40.72	48.41	36.91	224.40	5.30
7	105.36	− 11.60	112.05	− 10.88	42.93	30.17	44.45	25.71	220.40	3.43
8	105.32	− 11.63	112.05	− 10.88	42.43	28.65	43.98	24.38	218.00	2.30
9	105.34	− 11.61	112.18	− 10.78	45.29	37.33	46.64	31.90	221.20	3.80
10	105.35	− 11.60	112.18	− 10.78	43.05	30.53	45.02	27.32	219.00	2.77
11	105.37	− 11.59	111.90	− 11.00	43.43	31.69	44.87	26.89	218.90	2.72
12	105.34	− 11.61	111.85	− 11.04	42.18	27.90	43.64	23.42	217.20	1.92
13	105.37	− 11.59	111.93	− 10.98	39.70	20.38	41.42	17.14	212.00	− 0.52
14	105.36	− 11.60	111.93	− 10.98	41.81	26.77	43.20	22.17	214.90	0.84
15	105.39	− 11.57	111.93	− 10.98	51.38	55.79	52.55	48.61	228.10	7.04
16	105.39	− 11.57	111.68	− 11.17	43.68	32.44	45.03	27.35	216.80	1.74
17	117.81	− 1.15	125.10	− 0.50	48.03	45.63	49.55	40.13	223.00	4.65
18	105.38	− 11.58	111.68	− 11.17	44.79	35.81	46.33	31.02	218.30	2.44
19	105.37	− 11.59	111.93	− 10.98	36.84	11.70	37.85	7.04	208.40	− 2.21
20	105.36	− 11.60	111.80	− 11.08	46.16	39.96	47.29	33.74	221.30	3.85

Table 4 Melting range, solidification range and enthalpy of solidification of In-48Sn obtained for each thermal cycle on the DSC

Cycle no.	$T_{m,\ onset}$ (°C)	RPD (%)	$T_{m,\ peak}$ (°C)	RPD (%)	$T_{s,\ onset}$ (°C)	RPD (%)	$T_{s,\ peak}$ (°C)	RPD (%)	ΔH_s (J/g)	RPD (%)
1	117.65	–	121.74	–	112.98	–	112.47	–	22.82	–
2	117.27	− 0.32	120.26	− 1.22	112.80	− 0.16	112.46	− 0.01	21.50	− 5.78
3	117.15	− 0.42	120.31	− 1.17	112.92	− 0.05	112.58	0.10	21.56	− 5.52
4	117.27	− 0.32	120.28	− 1.20	112.92	− 0.05	112.68	0.19	21.44	− 6.05
5	117.27	− 0.32	120.29	− 1.19	112.92	− 0.05	112.60	0.12	22.12	− 3.07
6	117.40	− 0.21	120.48	− 1.03	113.42	0.39	112.87	0.36	21.06	− 7.71
7	117.40	− 0.21	120.46	− 1.05	113.29	0.27	112.89	0.37	21.29	− 6.70
8	117.40	− 0.21	120.62	− 0.92	113.29	0.27	112.88	0.36	21.30	− 6.66
9	118.05	0.34	120.60	− 0.94	113.42	0.39	112.85	0.34	21.36	-6.40
10	117.40	− 0.21	120.63	− 0.91	113.32	0.30	112.83	0.32	21.23	− 6.97
11	117.27	− 0.32	120.77	− 0.80	113.28	0.27	112.77	0.27	21.25	− 6.88
12	117.40	− 0.21	120.75	− 0.81	113.12	0.12	112.63	0.14	21.32	− 6.57
13	117.02	− 0.54	120.77	− 0.80	113.43	0.40	112.85	0.34	21.13	− 7.41
14	117.27	− 0.32	120.91	− 0.68	113.08	0.09	112.58	0.10	21.00	− 7.98
15	117.27	− 0.32	120.92	− 0.67	113.24	0.23	112.67	0.18	20.87	− 8.55
16	117.15	− 0.42	120.90	− 0.69	113.10	0.11	112.53	0.05	21.41	− 6.18
17	117.27	− 0.32	120.93	− 0.67	113.16	0.16	112.61	0.12	21.34	− 6.49
18	117.40	− 0.21	120.96	− 0.64	113.07	0.08	112.56	0.08	21.32	− 6.57
19	117.40	− 0.21	120.77	− 0.80	113.17	0.17	112.65	0.16	21.18	− 7.19
20	117.40	− 0.21	120.78	− 0.79	113.07	0.08	112.54	0.06	21.22	− 7.01

show quick responses to the large drop in the melting temperature noticed in cycle 2 and cycle 18. Significant responses were only noticeable in the next solidification cycle after the cycles where the transformations took place. These variations in the solidification onset and peak temperatures are responsible for the scattered solidification peaks noticeable on the DSC thermogram (Fig. 2b). However, there is no clear effect of the switches between the stable state and the metastable state on the solidification enthalpy. Meso-erythritol exhibits large degrees of supercooling between 54.01 and 86.20 °C as observed during the 20 heating and solidification cycles. The variations in the solidification enthalpy of − 2.21 and + 5.3% of the initial value of 213.10 J/g did not show any particular trend. The solidification enthalpy can be taken to be reasonably stable over the 20 heating/solidification cycles.

As observable from Table 4, In-48Sn showed slight variations in its melting onset temperature of between − 0.21 and− 0.54% of the value of 117.65 °C in cycle 1 with no particular trend. Variations of between − 0.64 and − 1.22% of the initial value of 121.74 °C were obtained for the solidification peak temperature. The solidification onset temperature varied between − 0.16 and + 0.4% of the initial value of 112.98 °C in cycle 1. Slight variations of between − 0.01 and + 0.37% of an initial value of 112.47 °C were also obtained for the solidification enthalpy temperature. The solidification enthalpy varied between − 8.55 and − 3.07% from the initial value of 22.82 J/g. The melting onset and peak temperatures, solidification onset and peak temperatures and the solidification enthalpy of In-48Sn are reasonably stable through the 20 heating/solidification cycles. In-48Sn exhibited very low degrees of supercooling of between 4.17 and 5.20 °C.

3.3 Thermal cycling tests—TGA

Table 5 shows the results obtained from simultaneous TGA with the thermal cycling of acetanilide, meso-erythritol and In-48Sn at heating/cooling rates of 20 °C/min. Acetanilide was thermally cycled between 35 and 130 °C, meso-erythritol between 20 and 140 °C and In-48Sn between 35 and 140 °C. Though the maximum heating temperature for each PCM was kept below its earlier observed decomposition temperature, acetanilide showed almost constant rapid rate of degrading per cycle. After 20 cycles, only 41.17% of the original weight of the acetanilide sample was left. The mass degradation of the PCMs is responsible for the noticeable progressive decrease in the DSC heat-flow peaks for the PCMs (Fig. 2a–c). Meso-erythritol showed slower rate of degrading per cycle, with 95.28% of the original weight of the sample left after 20 thermal cycles. The best performance was shown by In-48Sn with

Table 5 Percentage of the initial weight of acetanilide, meso-erythritol and In-48Sn left after each thermal cycle

Cycle no.	Acetanilide % weight	Meso-erythritol % weight	In-48Sn % weight
1	96.57	98.63	99.66
2	93.66	98.46	99.57
3	90.64	98.34	99.51
4	87.76	98.14	99.46
5	85.07	97.99	99.41
6	82.03	97.83	99.37
7	79.20	97.62	99.37
8	76.09	97.46	99.31
9	73.20	97.29	99.27
10	70.30	97.29	99.23
11	67.31	96.96	99.19
12	64.39	96.75	99.15
13	61.45	96.54	99.12
14	58.50	96.32	99.10
15	55.56	96.11	99.08
16	52.69	95.93	99.06
17	49.78	95.75	99.04
18	46.91	95.58	99.03
19	44.03	95.44	99.02
20	41.17	95.28	99.01

99.01% of its original weight remaining after the thermal cycles.

3.4 Chemical stability

In order to investigate the chemical stabilities of the PCMs in this study, the FTIR spectra of three PCMs were obtained prior to and after the 20 thermal cycles. Figure 3a–c shows the infrared spectra obtained for fresh sample and the residue of each PCM after the thermal cycles. The infrared spectrum obtained before thermal cycling shows similar peak profile with that obtained from the fresh sample for each of the PCM.

This is an indication that the residue of each PCM, after thermal cycling, possesses the same chemical structure as the original material. It is noteworthy that the metastability exhibited by meso-erythritol was not observable from the spectra obtained from the meso-erythritol residue as it might have gone into its stable crystalline form due to the time lag in transferring the residue from the DSC equipment to the FTIR equipment.

3.5 Health hazard

Table 6 shows the health hazard ratings for acetanilide, meso-erythritol and In-48Sn according to the National Fire Protection Association (NFPA) rating system. The NFPA 704 blue diamond is a standard system for identification of health hazards of materials for emergency response. The grading is from 0 to 4, where 0 indicates substances that present very minimal hazards to health and 4 indicates substances that could cause severe hazard or death with short exposure.

Exposure of the eyes and skin to acetanilide may cause irritation while ingestion/inhalation may cause irritation of the digestive tract, damage to the liver, cyanosis, convulsions and death, when ingested [37]. Therefore, great care must be taken while handling, encapsulating and using acetanilide to avoid contact with skin, inhalation of its dust/fumes and ingestion. Meso-erythritol may cause mild skin and eye irritation and may also cause irritation to the respiratory tracts [33]. Some care should be taken during handling and encapsulation of this PCM. Inhalation of In-48Sn fumes may cause irritation to the respiratory system and may additionally cause headache, nausea, abdominal pain and also pain in the legs, arms and joints. The fumes or the powder of this alloy may cause eye irritation and its indigestion may cause irritation/damage to the digestive tracts [34]. Care must be taken while encapsulating In-48Sn so as not to inhale its fumes and ingestion of the alloy should be avoided. The potential health hazards for the three materials are low as long as highlighted minimal safety precautions are taken. They may therefore be utilized as PCMs for cooking applications safely while concealed (encapsulated).

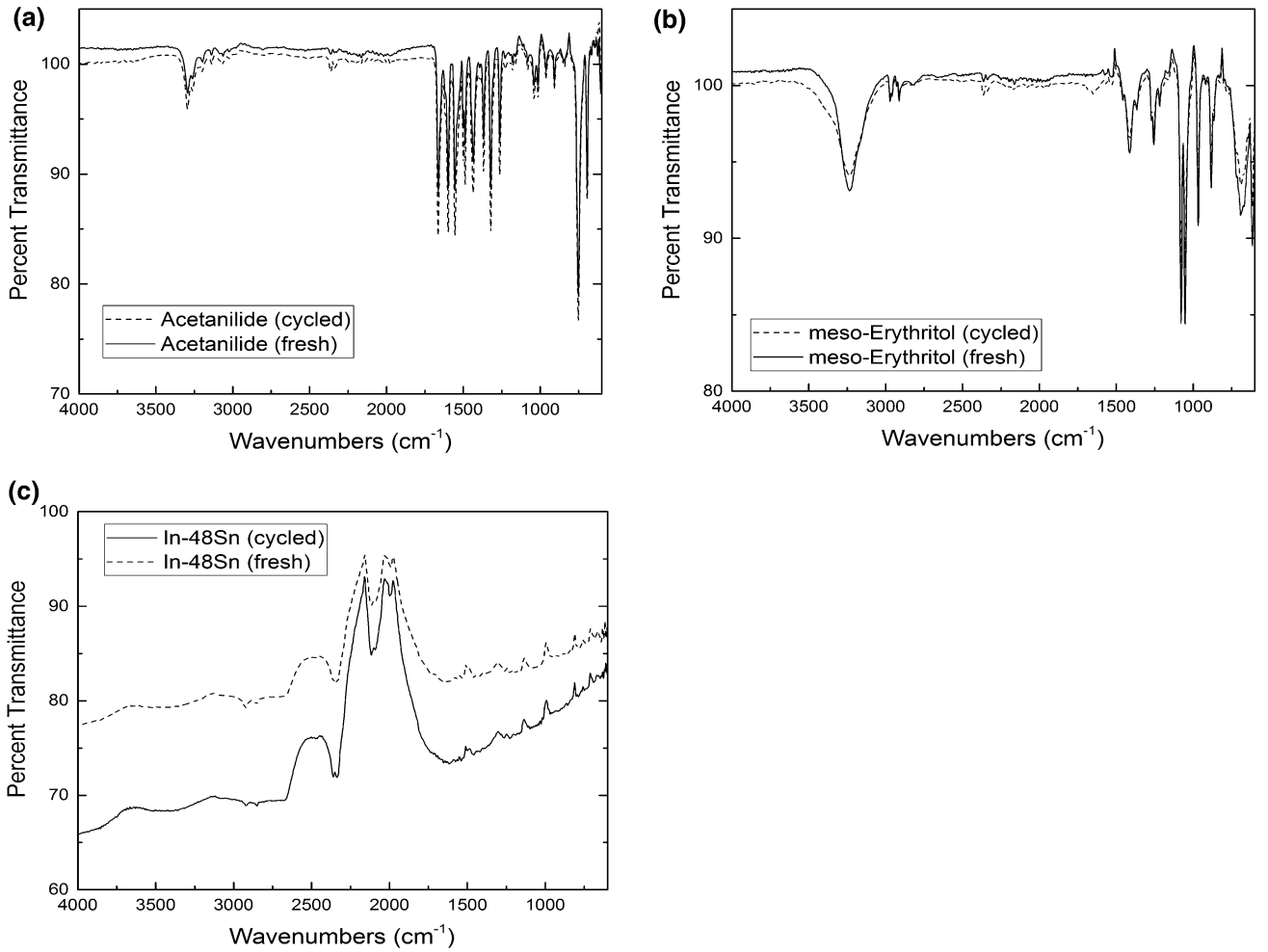

Fig. 3 Infrared spectra obtained for fresh and cycled samples of **a** acetanilide, **b** meso-erythritol and **c** In-48Sn

Table 6 NFPA health hazard ratings for acetanilide, meso-erythritol and In-48Sn

PCM	Health hazard (NFPA)
Acetanilide	2 [22]
Meso-erythritol	1 [23]
In-48Sn	2 [24]

3.6 Thermal storage capacity

From Table 7, it can be observed that In-48Sn will present a thermal mass per unit volume which is about five times that presented by meso-erythritol and six times that presented by acetanilide due to its larger density.

Based on the data in Table 7, it can be estimated that the volumetric heat capacity of acetanilide is about 2420 J/m^3 K, for meso-erythritol it is about 2042.4 J/m^3 K (solid) and 4084.8 J/m^3 K (liquid) while for In-48Sn it is about 1693.9 J/K (solid) and 3024.3 J/K (liquid). Based on the average values of the enthalpies of solidification of acetanilide, meso-erythritol and In-48Sn, the volumetric enthalpies of solidification are estimated to yield 170 041.3 J/m^3 for acetanilide, 323 875.8 J/m^3 for meso-erythritol and 155 476.2 J/m^3 for In-48Sn. In-48Sn, however, possesses the highest values of thermal conductivity and thermal diffusivity in both solid and liquid phases. The estimated thermal diffusivity value is 0.05 mm^2/s for acetanilide, 1.29 mm^2/s and 0.33 mm^2/s for solid and liquid meso-erythritol, respectively, while it is 24.16 and 21.12 mm^2/s for solid and liquid In-48Sn, respectively. The rates of charging and discharging of LHTES units have been reported to be influenced by the thermal diffusivity of the PCM used.

3.7 Cost

The cost implications of the three PCMs are shown in Table 8, where the volumes are determined based on the

Table 7 Some other thermophysical properties of acetanilide, meso-erythritol and In-48Sn

Property	Acetanilide	Meso-erythritol	In-48Sn
Density (kg/m^3)	1210 [7]	1480 (20 °C) [17]	7270 (20 °C)[a]
		1300 (140 °C) [17]	7060 (140 °C)[a]
Specific heat capacity (kJ/kg K)	2.00 [6]	1.38 (20 °C) [17]	0.233 (30 °C)[a]
		2.76 (140 °C) [17]	0.416 (120 °C)[a]
Thermal conductivity (W/m K)	0.13 [36]	2.64 (20 °C) [17]	40.92(30 °C)[a]
		1.17 (140 °C) [17]	62.02 (120 °C)[a]

[a]Measured values

Table 8 The cost of the acetanilide, meso-erythritol and In-48Sn samples used in this study

PCM	Unit cost (US $/kg)	Estimated cost per unit volume (US $/$m^3$)	Cost per unit thermal energy (sensible + latent) (US $/kJ)	Cost per unit thermal energy (latent) (US $/kJ)
Acetanilide	113.00	136,730.00	0.32	0.81
Meso-erythritol	36.80	54,464.00	0.21	0.17
In-48Sn	758.84	5,516,766.80	6.58	35.48

densities in Table 7. In-48Sn is shown to have the highest cost per unit volume which is about forty times the cost of acetanilide and about one hundred times the cost of meso-erythritol per unit volume. Meso-erythritol clearly presents the cheapest cost per unit volume.

The cost of unit thermal energy deliverable by each of the PCM in a single heating/cooling cycle was calculated assuming that each PCM was initially charged up to the observed decomposition temperature (T_d) and allowed to cool to 25 °C.

The cost of both sensible heat thermal energy and latent heat deliverable was calculated by:

$$\text{Cost/Energy}(\text{US\$/kJ}) = \frac{\text{Cost of 1 kg of PCM}}{(T_d - T_{s,onset})c_l + \Delta H_s + (T_{s,peak} - 25)c_s} \quad (1)$$

And the cost of the latent heat thermal energy deliverable was calculated by:

$$\text{Cost/Energy}(\text{US\$/kJ}) = \frac{\text{Cost of 1 kg of PCM}}{\Delta H_s} \quad (2)$$

The values of the solidification onset and peak temperatures as well as the solidification enthalpy for each PCM used for calculations were average values obtained from the thermal cycling experiment.

From Table 8, it can be observed that the cheapest unit cost of thermal energy deliverable is presented by meso-erythritol followed by acetanilide while that of In-48Sn is much higher. Based on cost consideration, meso-erythritol and then acetanilide would have been the preferred PCM but their solidification enthalpies are delivered at temperatures lower than desired cooking temperatures. From the thermal cycling experiments, meso-erythritol solidified averagely about 44.3–42.7 °C and acetanilide solidified averagely about 72.4–71.1 °C. In-48Sn, on the other hand, solidified averagely at about 112.6–113.2 °C which will make its delivered solidification enthalpy most suited for cooking applications.

4 Conclusions

The suitability of the use of acetanilide, meso-erythritol and In-48Sn as PCMs for thermal storage for cooking applications under fast charging and heat retrieval conditions has been investigated. In-48Sn showed good thermal stability up to about 289.68 °C which is much higher than operational temperatures that both acetanilide (133.0 °C) and meso-erythritol (177.0 °C) can be used. Acetanilide exhibited quite stable melting temperatures, solidification temperatures and solidification enthalpies with thermal cycling at 20 °C/min, but its mass was rapidly degraded with each cycle. While meso-erythritol showed large deviations in melting and solidification temperatures, the solidification enthalpy remained quite stable during thermal cycling at 20 °C/min. Some mass loss (4.72%) was also observed in the meso-erythritol sample after 20 cycles. The large variation in the melting temperature of meso-erythritol was due to a polymorphic transition into a metastable amorphous form with a lower melting temperature than its stable form, though this transition showed no effect on the enthalpy of solidification. In-48Sn showed

very good cycling stability with very little variation in its melting temperature, solidification temperature and solidification enthalpy. The alloy also showed very low degrees of supercooling of between 4.17 and 5.20 °C and the least mass degradation (0.99%) after 20 rapid heating/cooling cycles. Meso-erythritol possesses both the largest volumetric sensible heat capacity and volumetric solidification enthalpy followed by acetanilide and then In-48Sn. However, both acetanilide and meso-erythritol exhibited large degrees of supercooling to temperatures below 100 °C which is not desirable for effective cooking applications. Therefore, a mean of reducing supercooling is necessary in order to employ acetanilide and meso-erythritol in a thermal storage for cooking where rapid heat retrieval is required. The degrees of supercooling of the PCMs were probably very large due to the few milligrams of material required for measurements in the DSC/TGA equipment. Acetanilide, meso-erythritol and In-48Sn showed very good chemical stability after the rapid thermal cycles. The rapid mass degradation of acetanilide will discourage its use as it will present a LHTES rapidly diminishing thermal capacity and a short lifetime. The degrees of health hazard of the three PCMs are within acceptable limits though the PCMs should be pre-encapsulated in leakproof containments before use in order to avoid contact with food and the environment. Though In-48Sn possesses a low value of solidification enthalpy, it has a large density which gives it a considerable thermal mass. In-48Sn has promise as a PCM for cooking applications under high rates of heating and cooling but its high cost may hinder its use. However, the long-term cycling stability of In-48Sn may, however, be an advantage as there will be no need to replace PCM for a large number of heating/cooling cycles. Longer thermal cycling of In-48Sn will be undertaken in the future by the authors in order to establish the thermal reliability of the alloy over longer heating/solidification cycles. Cost–benefit analysis of using this metallic PCM compared to other alternative PCMs needs also be investigated using results from a long-term cycling experiment. Cheaper solder alloys need to be investigated in the near future as PCMs for cooking applications.

Acknowledgements The authors wish to acknowledge the support provided by the Material Science Innovation and Modeling (MaSIM) research focus area, Faculty of Natural and Agricultural Sciences at the North West University, South Africa. The authors also wish to acknowledge the National Research Foundation, South Africa, through the Incentive Funding for Rated Researchers (IFRR-Grant Nos.: 90638, 95574) scheme.

References

1. Fernandes D, Pitie F, Caceres G, Baeyens J (2012) Thermal energy storage: "How previous findings determine current research priorities". Energy 39:246–257
2. Sharma A, Tygi VV, Chen CR, Buddhi D (2009) Review on thermal energy storage with phase change materials and application. Renew Sustain Energy Rev 13:318–345
3. Miro L, Barreneche C, Ferrer G, Sole A, Martorell I (2016) Health hazard, cycling and thermal stability as key parameters when selecting a suitable phase change material (PCM). Thermochim Acta 627–629:39–47
4. Muthusivagami RM, Velraj R, Sethumadhavan R (2010) Solar cookers with and without thermal storage—a review. Renew Sustain Energy Rev 14:691–701
5. Sharma SD, Buddhi D, Sawhney RL, Sharma A (2000) Design, development and performance evaluation of a latent heat storage unit for evening cooking in a solar cooker. Energy Convers Manag 41(14):1497–1508
6. Domanski R, El-Sebaii AA, Jaworski M (1995) Cooking during off-sunshine hours using PCMs as storage media. Energy 20(7):607–616
7. Choudhari KS, Shende MD (2015) Solar cooker using PCM material. J Basic Appl Eng Res 2(17):1449–1453
8. Saxena A, Lath S, Tirth V (2013) Solar cooking by using PCM as a thermal heat storage. MIT Int J Mech Eng 3(2):91–95
9. Buddhi D, Sharma SD, Sharma A (2003) Thermal performance evaluation of a latent heat storage unit for late evening cooking in a solar cooker having three reflectors. Energy Convers Manag 44:809–817
10. Sharma SD, Iwata T, Kitano H, Sagara K (2005) Thermal performance of a solar cooker based on an evacuated tube solar collector with a PCM storage unit. Sol Energy 78:416–426
11. Hussein HMS, El-Ghetany HH, Nada SA (2008) Experimental investigation of novel indirect solar cooker with indoor PCM thermal storage and cooking unit. Energy Convers Manag 49:2237–2246
12. Mussard M, Gueno A, Nydal OJ (2013) Experimental study of solar cooking using heat storage in comparison with direct heating. Sol Energy 98:375–383
13. Lecuona A, Nogueira J, Ventas R, Rodríguez-Hidalgo M, Legrand M (2013) Solar cooker of the portable parabolic type incorporating heat storage based on PCM. Appl Energy 111:1136–1146
14. Nandwani SS (1997) Experimental study of multipurpose solar hot box at Freiburg, Germany. Renew Energy 12(1):1–20
15. Buddhi D, Sahoo LK (1997) Solar cooker with latent heat storage: design and experimental testing. Energy Convers Manag 38(5):493–498
16. Liu Z, Chung DDL (2001) Calorimetric evaluation of phase change materials for use as thermal interface materials. Thermochimita Acta 366:135–147
17. Ge H, Li H, Mei S, Liu J (2013) Low melting point liquid metal as a new class of phase change material: an emerging frontier in energy area. Renew Sustain Energy Rev 21:331–346
18. Kotzé JP, von Backström TW (2013) High temperature thermal energy storage utilizing metallic phase change materials and metallic heat transfer fluids. J Sol Energy Eng 135:035001
19. Kenisarin M, Mahkamov K (2007) Solar energy storage using phase change materials. Renew Sustain Energy Rev 11:1913–1965
20. Sharma SD, Sagara K (2005) Latent heat storage materials and systems: a review. Int J Green Energy 2:1–56

21. Saini P, Sharma V, Singh C (2014) Performance evaluation of thermal storage unit based on parabolic dish collector for indoor cooking application. J Acad Ind Res 3(7):304–310
22. El-Sebaii AA, Al-Amir S, Al-Marzouki FM, Faidah AS, Al-Ghamdi AA, Al-Heniti S (2009) Fast thermal cycling of acetanilide and magnesium chloride hexahydrate for indoor solar cooking. Energy Convers Manag 50:3104–3111
23. El-Sabaii AA, Al-Agel F (2012) Fast thermal cycling of acetanilide as a storage material for solar energy applications. ASME J Sol Energy Eng 135(2):024502
24. Gunasekara SN, Pan R, Chiu JN, Martin V (2014) Polyols as phase change materials for low-grade excess heat storage. Energy Procedia 61:664–669
25. Kaizawa A, Marouka N, Kawai A, Kamano H, Jozuka T, Senda T, Akiyama T (2008) Thermophysical and heat transfer properties of phase change material candidate for waste heat transportation system. Heat Mass Transf 44:763–769
26. Agyenim F, Rhodes M, Knight I (2007) The use of phase change material (PCM) to improve the coefficient of performance of a chiller for meeting domestic cooling in Wales. In: Proceedings of 2nd PALENC conference and 28th AIVC conference on building low energy cooling and advanced technologies in the 21st century, Crete Island
27. Puupponen S, Mikkola V, Ala-Nissila T, Seppala A (2016) Novel microstructured polyol-polystrene composite for seasonal heat storage. Appl Energy 172:96–106
28. Nomura T, Tsubota M, Oya T, Okinaka N, Akiyama T (2013) Heat release performance of direct-contact heat exchanger with erythritol as phase change material. Appl Therm Eng 61:28–35
29. Kakiuchi H, Yamazaki M, Yabe M, Chihara S, Terunuma Y, Sakata Y, Usami T (1998) A study of Erythritol as phase change material, In: Chemical Engineering and Technology, Royal Institute of Technology. IEA Annex 10-PCMs and chemical reactions for thermal energy storage, second workshop, Sofia
30. Shukla A, Buddhi D, Sawhney RL (2008) Thermal cycling test of few selected inorganic and organic phase change materials. Renew Energy 33:2606–2614
31. Myers B, Chaudhuri AK, Burns JH (2003) Thermally-capacitive phase change encapsulant for electronic devices, US Patent; US20030157342; 2003
32. https://www.alfa.com/en/content/msds/USA/A14361.pdf. Accessed 11.08.16
33. http://www.jk-scientific.com/Product/ProductDetails/4241?categoryid=793. Accessed 11.08.16
34. http://www.indium.com/technical-documents/safety-data-sheets/european/. Accessed 12.08.16
35. Jesus AJL, Nunes SCC, Silva M, Beja AM, Redinha JS (2010) Erythritol: crystal growth from melt. Int J Pharm 388:129–135
36. Yaws CL (1995) Handbook of Thermal conductivity, organic compounds C_8 to C_{28}. Gulf Publishing Company, Houston
37. http://www.clayton.edu/portals/690/chemistry/inventory/MSDS%20Acetanilide.pdf. Accessed 27.03.2018